RESEARCH ARTICLE

Transcriptome sequencing reveals *maelstrom* as a novel target gene of the terminal system in the red flour beetle *Tribolium castaneum*

Fabian Pridöhl[1], Matthias Weißkopf[1], Nikolaus Koniszewski[1,*], Andreas Sulzmaier[1], Steffen Uebe[2], Arif B. Ekici[2] and Michael Schoppmeier[1,‡]

ABSTRACT

Terminal regions of the *Drosophila* embryo are patterned by the localized activation of the Torso-RTK pathway, which promotes the downregulation of Capicua. In the short-germ beetle *Tribolium*, the function of the terminal system appears to be rather different, as the pathway promotes axis elongation and, in addition, is required for patterning the extra-embryonic serosa at the anterior. Here, we show that Torso signalling also induces gene expression by relieving Capicua-mediated repression in *Tribolium*. Given that the majority of Torso target genes remain to be identified, we established a differential gene-expression screen. A subset of 50 putative terminal target genes was screened for functions in early embryonic patterning. Of those, 13 genes show early terminal expression domains and also phenotypes were related to terminal patterning. Among others, we found the PIWI-interacting RNA factor Maelstrom to be crucial for early embryonic polarization. *Tc-mael* is required for proper serosal size regulation and head morphogenesis. Moreover, *Tc-mael* promotes growth-zone formation and axis elongation. Our results suggest that posterior patterning by Torso may be realized through Maelstrom-dependent activation of posterior Wnt domains.

KEY WORDS: *Tribolium*, **Short-germ insect, Terminal system, Anterior-posterior patterning, Transcriptome sequencing**, *Torso*, *Torso-like, Capicua, Maelstrom*

INTRODUCTION

Anterior-posterior patterning of the *Drosophila* embryo depends on spatial polarity cues provided by maternal coordinate systems (St Johnston and Nüsslein-Volhard, 1992). While anterior patterning is mediated by the Bicoid morphogen (Driever and Nüsslein-Volhard, 1988), posterior patterning largely depends on Nanos (Nos) and Pumilio (Pum) proteins (Barker et al., 1992; Macdonald, 1992; Nüsslein-Volhard et al., 1987; Wang and Lehmann, 1991). The terminal system acts to pattern the anterior and posterior non-segmented regions of the embryo through the *torso*-mediated receptor tyrosine kinase (Ras/MAPK) pathway

[1]Department of Biology, Developmental Biology Unit, Friedrich-Alexander-University Erlangen-Nuremberg, Staudtstrasse 5, Erlangen 91058, Germany. [2]Institute of Human Genetics, Friedrich-Alexander-University Erlangen-Nuremberg, Schwabachanlage 10, Erlangen 91054, Germany. *Present address: Institut für Medizinische Mikrobiologie und Krankenhaushygiene, Otto-von-Guericke-University, Leipziger Strasse 44, Magdeburg 39120, Germany.

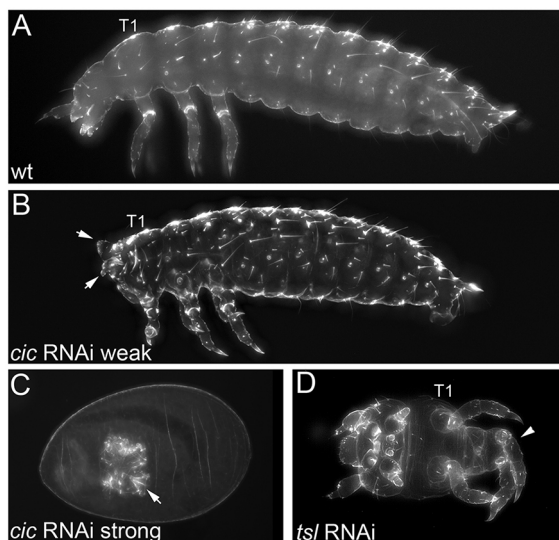‡Author for correspondence (michael.schoppmeier@fau.de)

M.S., 0000-0002-6143-8802

(Furriols and Casanova, 2003; Li, 2005). Both Torso receptor and its putative ligand Trunk are ubiquitously expressed throughout the oocyte, and it appears that localized Torso activation results from activation of Trunk by Torso-like, the expression of which is restricted to ovarian follicle cells (Johnson et al., 2015; Mineo et al., 2015; Savant-Bhonsale and Montell, 1993; Stevens et al., 2003). Stimulation of Torso signalling results in de-repression of the terminal target genes *tailless* (*tll*) and *huckebein* (*hkb*). This activation is indirect and involves de-repression mechanisms. Terminal target genes are usually repressed and the activation of Torso relieves this repression, which allows *tll* and *hkb* expression at the poles of the embryo. Repression of terminal target genes requires the high-mobility group (HMG) protein Capicua (Cic) and the Groucho (Gro), which acts as a co-repressor. In absence of maternal Cic, *tll* and *hkb* are de-repressed and expression expands towards central regions of the embryo. This results in the loss of thoracic and abdominal anlagen (Ajuria et al., 2011; Astigarraga et al., 2007; de las Heras and Casanova, 2006; Jimenez et al., 2000; Liaw and Lengyel, 1993; Paroush et al., 1997).

The red flour beetle *Tribolium* develops as a short-germ embryo. The majority of segments get patterned in a secondary growth process from a so-called growth zone (Klingler, 2004; Richards et al., 2008). At the blastoderm stage, the anterior region of the *Tribolium* egg gives rise to extra-embryonic serosa and amnion, whereas embryonic anlagen are restricted towards the ventral-posterior region of the egg (Handel et al., 2000).

Despite these differences, Torso-signalling was shown to be active at both poles of the *Tribolium* egg (Schoppmeier and Schröder, 2005; Schroder et al., 2000). At the posterior, Torso is required for setting up or maintaining a functional growth zone. In the absence of Torso signalling, invagination fails and embryos are depleted of all growth zone-derived segments (Grillo et al., 2012; Schoppmeier and Schröder, 2005). At the anterior, terminal signalling is crucial for the formation of extra-embryonic membranes. In *Torso* or *tsl* RNAi, the serosa is reduced in size (Schoppmeier and Schröder, 2005; van der Zee et al., 2005).

Although the putative target genes of the *Tribolium* Torso pathway in the anterior region remain to be identified, posterior expression of *Tc-wingless* (*Tc-wg*), *Tc-tailless* (*Tc-tll*), *Tc-caudal* (*Tc-cad*) and *Tc-forkhead* (*Tc-fkh*) depends on Tor activation (Schoppmeier and Schröder, 2005). Yet Torso RNAi phenotypes cannot be entirely explained by the loss of the known target genes, indicating that crucial components for terminal patterning remain to be identified (Casanova, 2005). By comparing terminal-system loss-of-function (*Tc-tsl* RNAi) and gain-of-function (*Tc-cic* RNAi) transcriptomes with the wild-type transcriptome, we have identified the first comprehensive set of Tor-target genes in a short-germ insect.

RESULTS

Capicua acts as a repressor of Torso target genes in *Tribolium*

To elucidate, whether Capicua fulfils a conserved function in repressing Torso target-genes, we characterized the *Tribolium capicua* ortholog (*Tc-cic*, TC004697). *Tc-cic* mRNA is expressed ubiquitously in unfertilized eggs and is also present in early blastoderm embryos (not shown), thus resembling the situation in *Drosophila* (Jimenez et al., 2000). Depletion of *Tc-cic* by parental RNAi results in severe patterning defects (Fig. 1; Fig. S1). Only about 7% of eggs collected in the first week after eclosion of injected animals were capable of secreting a larval cuticle, whereas 92.4% of the embryos die prior to completion of embryonic development (empty egg) (Schmitt-Engel et al., 2015). To determine whether or not the strong *Tc-cic* RNAi no-cuticle phenotype reflects a late function in maintaining embryonic anlagen, we performed time-lapse recordings of live embryos using a transgenic line expressing nuclear-localized GFP driven by the *Tribolium*EF1-α promoter (EFA-nGFP) (Sarrazin et al., 2012) (Fig. 2; Movies 1 and 2).

In wild-type embryos, at the differentiated blastoderm stage, a clear distinction arises between the wider-spaced serosal cells and the more densely spaced cells of the germ rudiment (Fig. 2A; Movie 1) (Handel et al., 2000). During gastrulation, embryonic anlagen condense and give rise to the germ rudiment that progressively becomes covered by the extending extra-embryonic membranes (i.e. serosa and amnion) (Fig. 2E,G; Movie 1) (Benton et al., 2013; Handel et al., 2000). Eventually, the head anlagen become morphologically visible, serosa window closure proceeds and germ-band elongation can be observed (Benton et al., 2013; Handel et al., 2000) (Movie 1).

Upon *Tc-cic* RNAi, extra-embryonic membranes are enlarged and expanded towards the posterior pole of the embryo (Fig. 2B,D; Movie 2). During gastrulation, the serosal cells spread in a posterior direction, while the residual embryonic tissue invaginates (Fig. 2F).

Eventually, extra-embryonic membranes cover the entire egg, while embryonic tissue is restricted to the posterior pole of the egg and becomes internalized completely. This presumably embryonic tissue does not show any signs of morphological differentiation or axis elongation (Fig. 2H; Movie 2). At this point, embryonic development stops. Thus, the majority of *Tc-cic* depleted embryos die during or soon after gastrulation.

To analyse early patterning of the serosa anlage, we stained *Tc-cic* RNAi embryos for *zerknüllt-1* (*Tc-zen-1*), which in wild type is already expressed in the presumptive serosa (Fig. 3G) (Falciani et al., 1996). As expected, in *Tc-cic*-depleted embryos the *Tc-zen-1* expression expands towards the posterior, indicating that the serosa primordium is already enlarged (Fig. 3I). Interestingly, the serosa-embryo boundary in the differentiated blastoderm is still oblique in *Tc-cic* RNAi (Fig. 3), suggesting that *Tribolium* Cic may have no impact on embryonic DV patterning.

In order to reveal the function of *Tc-cic* in patterning gnathal and thoracic anlagen, we analysed the formation of segment primordia by *Tc-even-skipped* (*eve*) expression (Fig. 3A-F). In the blastoderm, the pair-rule gene *Tc-eve* is expressed in double-segmental stripes. Eventually, these primary domains will resolve into a segmental pattern (Patel et al., 1994; Schoppmeier and Schröder, 2005). *Tc-eve* stripe 1 correspond the maxillary primordia and *Tc-eve* stripe 2 covers the anlagen of the first thoracic segment. The third primary domain, however, resembles the anlagen of the posterior growth zone (Fig. 3B). In *Tc-cic* RNAi embryos, primary *Tc-eve* domains are still present, but are shifted towards the posterior pole of the embryo (Fig. 3C). In addition, the distance between *Tc-eve* stripe 1 and the serosa boundary is severely decreased in size, indicating the depletion of the pre-gnathal anlagen (Fig. 3F). This is supported by the loss of the ocular *Tc-wg* domain (Fig. 3L). In wild-type
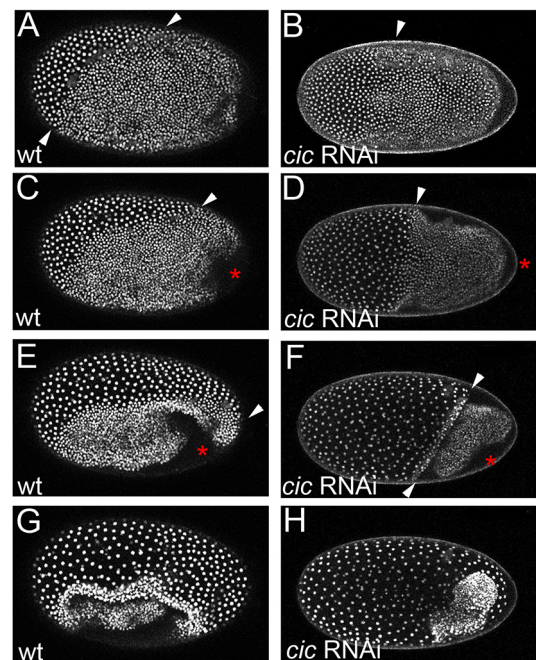

Fig. 1. Larval *Tc-capicua* and *Tc-torso-like* RNAi phenotypes. Cuticle of wild-type (A), and *Tc-cic* (B,C) and *Tc-tsl* (D) RNAi larvae. (B) Mildly affected *Tc-cic* RNAi larvae display head defects (arrows). (C) In strong phenotypes, cuticle remnants with urogomphile-like structures were obvious (arrow). (D) *Tc-tsl* RNAi larvae are depleted of growth zone-derived segments. The first thoracic segment (T1) is unaffected, T2 is reduced (arrowhead). Anterior is towards the left in all panels. (A,B) Lateral views; (C,D) ventral views.

Fig. 2. Live imaging of *Tc-cic* RNAi. Live imaging of wild-type and *Tc-cic* RNAi in the transgenic *Tribolium* EFA-nGFP line. Columns show nGFP-labelled stage-matched embryo at representative time-points. (A,C,E,G) Lateral views of wild-type embryos at differentiated blastoderm (A), posterior-pit (C), invagination (E) and serosa closure stages (G). (B,D,F,H) Corresponding stages of *Tc-cic* RNAi. Arrows indicate the serosa/embryo boundary, asterisks indicate the site of gastrulation.
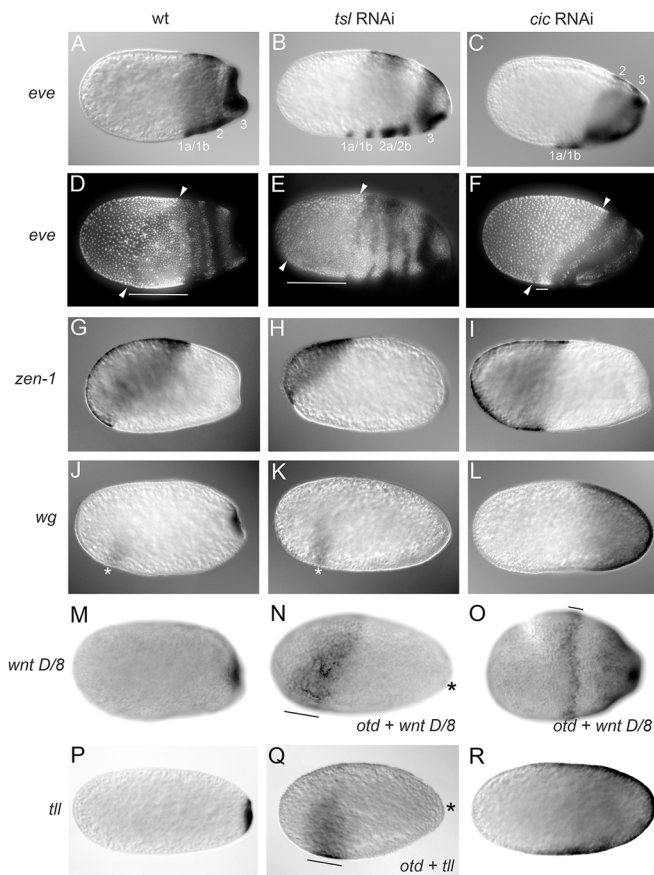
Fig. 3. Expression of terminal target genes in *Tc-cic* and *Tc-tsl* RNAi.
Expression of *Tc-eve* (A-C), *Tc-zen-1* (D-F), *Tc-wg* (J-L), *Tc-wnt D/8* (M-O) and *Tc-tll* (P-R) in wild-type (A,D,G,J,M,P), *Tc-tsl* (B,E,H,K,N,Q) and *Tc-cic* RNAi (C,F,I,L,O,R) embryos. Embryos in A-C were subsequently stained with the nuclear marker Hoechst 33342 (D-F). Embryos in N,O,Q were double stained for *Tc-otd* to visualize the head anlagen (bars). In wild type (A,B), *Tc-eve* is expressed in three primary stripes (1-3) that eventually split and give rise to segmental (1a, 1b) domains. In *Tc-tsl* RNAi (B,E), *Tc-eve* stripes are shifted toward the anterior, reflecting the expansion of the head anlagen (bar) at the expense of the serosa (arrowheads). In *Tc-cic*-depleted embryos (C,F), the serosa expands (arrowheads), while the head anlagen (bar) shrink. (G) *Tc-zen-1* is expressed in the anlagen of the serosa. (F,H) Upon *Tc-tsl* RNAi (H), *Tc-zen-1* expression reduced, while *Tc-zen-1* is expanded in *Tc-cic* RNAi (F). At the blastoderm stage, *Tc-wg* (J) is expressed in the ocular domain (asterisk) and at the posterior pole. In *Tc-tsl* RNAi (K), the posterior domain is absent. *Tc-cic* RNAi (L) results in the expansion of the posterior *Tc-wg* domain, while the head domain is lost. In wild-type blastoderm stages, *Tc-wnt D/8* and *Tc-tll* (M,P) are expressed at the posterior pole. After the knockdown of *Tc-tsl* (N,Q), *Tc-wnt D/8* and *Tc-tll* domains are absent (asterisk). *Tc-cic* RNAi (O,R) results in the expansion of both *Tc-wnt D/8* and *Tc-tll* domains.

blastoderm, *Tc-wg* is expressed in a posterior domain as well as in the ocular anlagen of the anterior head (Fig. 3J) (Nagy and Carroll, 1994). Upon *Tc-cic* knockdown, this anterior domain is no longer present (Fig. 3L). Thus, gnathal and anterior thoracic segments are initially patterned, whereas pre-gnathal segments apparently are lost.

Although *Tc-cic* RNAi causes the expansion of extra-embryonic membranes at the expense of the anterior head anlagen, the depletion of Torso signalling results in opposing effects (Fig. 3). In *Torso* or *tsl* RNAi, the serosa is reduced in size, while the presumptive head region appears enlarged and extended towards the anterior (Fig. 3E). This finding is corroborated by the expansion of *even-skipped* and the reduced expression of the serosal marker

zerknüllt-1 in *Tc-tsl* RNAi embryos (Schoppmeier and Schröder, 2005) (Fig. 3H). These phenotypes suggest that anterior *Tc-cic* RNAi reflects a de-repression phenotype of the terminal system.

Next, we tested whether posterior downstream gene activity is also affected in *Tc-cic* RNAi. To achieve this, we analysed the expression of *Tc-tll*, *Tc-wg* and *Tc-wntD/8* in early *Tc-cic* and *Tc-tsl* RNAi embryos (Fig. 3). In early wild-type blastoderm, *Tc-tll* is expressed in a small posterior domain (Fig. 3P) (Schroder et al., 2000). Whereas the posterior *tll* domain is abolished in *Tc-tsl* RNAi (Fig. 3Q), we observed a massive expansion of *Tc-tll* expression in *Tc-cic*-depleted embryos (Fig. 3R).

A de-repression phenotype was also observed for *Tribolium* Wnt genes (Fig. 3J-O). At the blastoderm stage, *wg/wnt1* and *wntD/8* are expressed at the posterior pole (Bolognesi et al., 2008a,b). In *Tc-tsl*, posterior *Tc-wg* and *Tc-wntD/8* domains are lost (Fig. 3K,N), indicating that posterior patterning by Torso may be realized, at least in part, through Wnt signalling. Again, the knockdown of *Tribolium cic* results in the expansion of posterior *Tc-wg* and *Tc-wntD/8* domains towards central regions of the embryo (Fig. 3L,O). Thus, as in *Drosophila* (Jimenez et al., 2000; Paroush et al., 1997), Torso signalling in *Tribolium* induces gene expression by relieving Cic-mediated repression.

Transcriptome sequencing and analysis of candidate genes

To uncover a comprehensive set of Torso target genes, we performed a differential gene-expression-screen, using next generation sequencing (NGS). To this end, we compared terminal-system loss-of-function (i.e. *Tc-tsl* RNAi) versus gain-of-function (i.e. *Tc-cic* RNAi) transcriptomes with the wild-type transcriptomes. Genes being differentially expressed in *Tc-tsl* versus *Tc-cic* RNAi (i.e. upregulated in *Tc-tsl* RNAi and downregulated in *Tc-cic* RNAi, or vice versa) likely depend on the activity of the terminal system.

Wild-type (T1), *tsl* RNAi (T2) and *cic* RNAi (T3) embryos were fixed at the differentiated blastoderm stage (7-11 h) and total RNA was isolated. Sequencing was carried out on a SOLiD 4 system (Life Technologies) and reads were mapped to the Tcas3 genome (http:// bioinf.uni-greifswald.de/gb2/gbrowse/tribolium/). In total, 12,795 genes showed differences in mRNA expression levels (Fig. 4 and Table S1). We found 1801 genes to be upregulated in *Tc-tsl* RNAi and downregulated in *Tc-cic* RNAi, and 2790 genes that were upregulated in *Tc-cic* RNAi but downregulated in *Tc-tsl* RNAi (see Table S1 for details).

Candidate genes for further inspection were selected by different criteria. To account for biological background variations, genes were only considered to be differentially expressed if the fold change (T1 versus T2 or T1 versus T3) was at least 50% compared with the wild type (*n*=2241), yet as the data was taken from a single technical replicate, comparisons of fold change numbers have statistically no significance value.

Expression of all differentially expressed genes was monitored by assessment of maternal and different early zygotic wild-type transcriptomes (M.S., unpublished, see http://bioinf.uni-greifswald. de/gb2/gbrowse/tribolium/). Genes were only taken into account if they were expressed during early stages of development (i.e. maternal until differentiated blastoderm), reducing the number of putative candidates to 1142. iBeetle phenotypes of candidates were monitored by comparison with the iB-database (http://ibeetle-base. uni-goettingen.de). The iBeetle screen was a large-scale RNAi screen *Tribolium*, which identified functions in embryonic and postembryonic development for more than half the *Tribolium* genes (Schmitt-Engel et al., 2015). Of the differentially expressed genes,
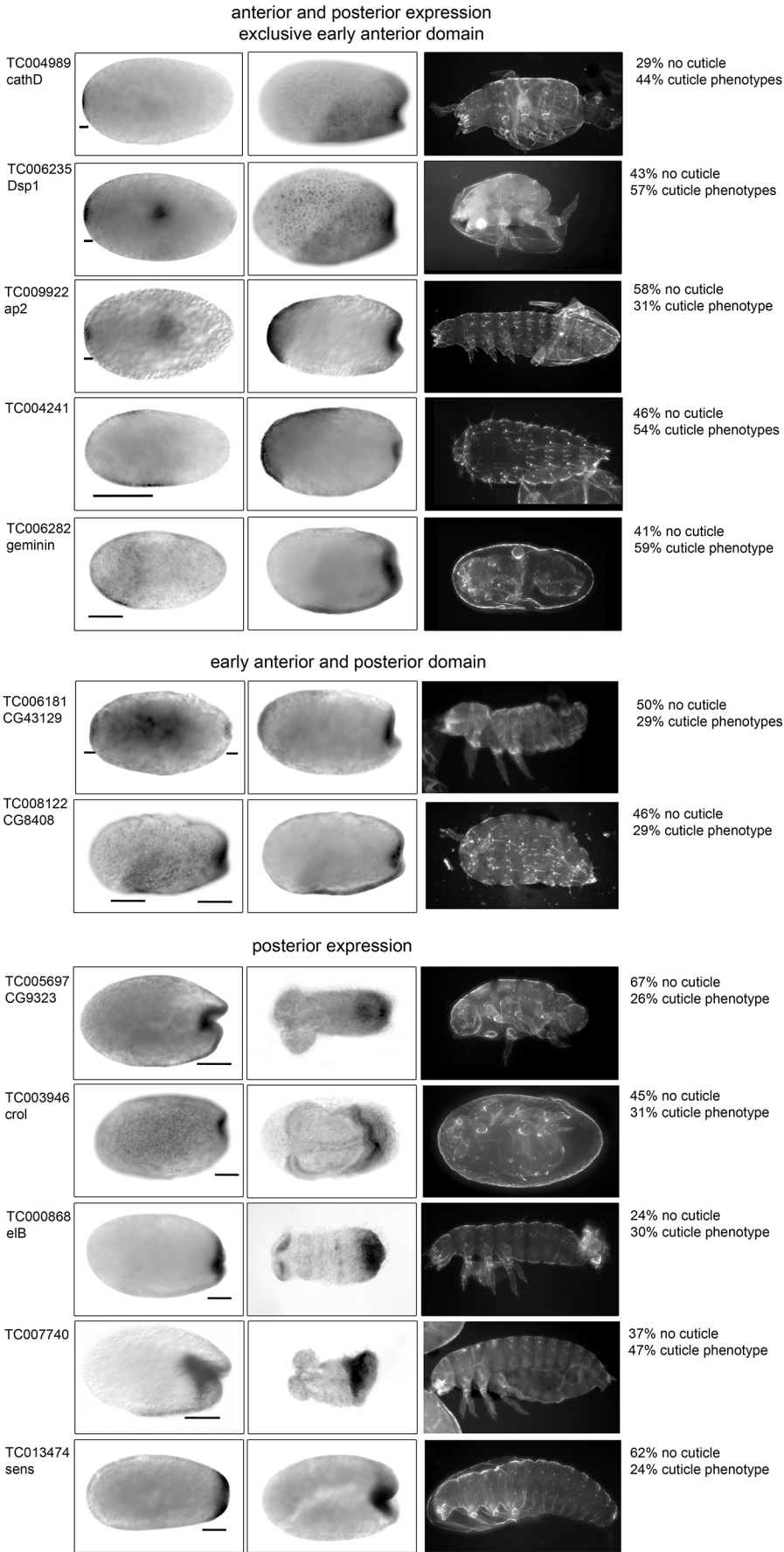
Fig. 4. Results of the RNAi and expression screen. Candidate genes were monitored for expression and function in AP patterning using RNAi. Depletion of genes resulted in larval phenotypes that, on most occasions, were associated with differing amounts of no-egg phenotypes.

more than 300 were represented in the iB-database. This comparison allowed us to exclude genes without any obvious embryonic/larval phenotype, as well as adult lethality, defects in metamorphosis and egg laying/oogenesis upon pupal RNAi. However, genes with larval phenotypes related to anterior-posterior patterning were preferentially selected for closer inspection, reducing the number of putative candidates to 122. In addition, *Drosophila* orthologs of all candidates were determined and candidates were classified according to their molecular and biological function (Table S2). Genes with no *Drosophila* orthologs or with unknown function were preferentially selected.

Based on these criteria, we selected 50 candidate genes and proceeded to screen those for functions in early patterning (Table S2). Larvae were scored for RNAi phenotypes. Phalloidin (f-actin) and Hoechst (DNA) staining was used to monitor embryonic phenotypes. In addition, expression was monitored by whole-mount *in-situ* hybridization (Table S2).

We found two genes that did not result in any detectable phenotype; five genes affected oogenesis, as we observed the cessation of egg-laying upon RNAi; and in 13 cases all eggs displayed no-cuticle phenotypes. As deduced from Hoechst and β-Tubulin staining, these so-called empty-egg phenotypes are due to lethality prior to cellularization (Table S2). Depletion of 30 genes resulted in larval phenotypes, which in most cases were associated with various quantities of empty-egg phenotypes (Table S2 and Fig. 4).

A single gene did not show any obvious expression at all and six genes were expressed only during later stages of development (i.e. germ-rudiment and subsequently). Thirty candidates were expressed ubiquitously during early stages (Table S2). Yet we identified 13 genes with distinct early terminal expression domains (Figs 4 and 5, see Table 1 for details).

Of these 13 candidate genes, five genes were exclusively expressed at the posterior pole or in the segment addition zone

(Fig. 4, Table 1). Eight of the 13 candidates were expressed at both poles at some point during embryonic development (Figs 4 and 5, Table 1). Interestingly, six out of these eight genes displayed an exclusive early anterior expression domain, either in freshly laid eggs (i.e. maternal expression, *TC004989*, *TC006235*, *TC009922* and *Tc-mael*) or in undifferentiated blastoderm stages (i.e. early zygotic expression, *TC004241* and *TC006282*), suggesting functions in patterning the anterior anlagen (Figs 4 and 5, Table 1).
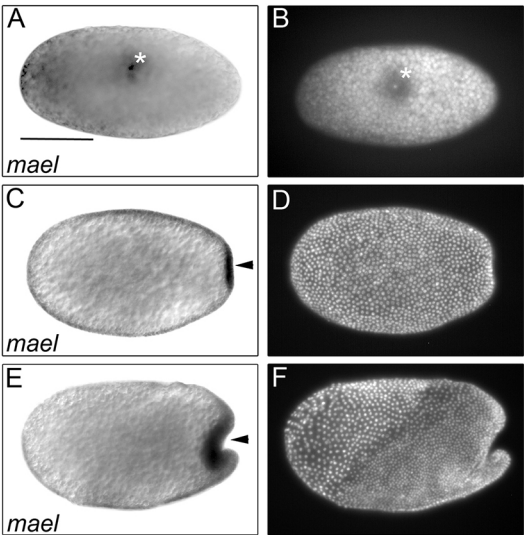
To control for potential off-target effects, we tested these 13 genes by injecting dsRNA fragments not overlapping with the original dsRNA fragments ('non-overlapping fragments', NOFs). All phenotypes were identical to those observed for the original dsRNA fragments (not shown).

Larval phenotypes are correlated with the expression of the candidates: genes being expressed at the posterior pole predominantly display posterior truncations or aberrations (Fig. 4, Table 1). For example, larvae depleted for *TC004989*, *TC005697* or *TC003946* show the loss of abdominal segments, as seen after loss of Torso-signalling (Schoppmeier and Schröder, 2005) and RNAi with *TC000868* and *TC013474* results in the depletion of terminal structures (i.e. urogomphi and pygopods). Candidates that are also expressed anteriorly frequently show additional head defects. The knockdown of *TC006181* or *TC006282* not only affects axis

Fig. 5. Expression of *Tc-mael*. (A-F) Expression of *Tc-mael*. Embryos in A,C, E were subsequently stained with Hoechst 33342 (B,D,F). (A,B) In unfertilized eggs, *Tc-mael* is expressed around the polar body (asterisks) and in an anterior domain of the embryo (bar in A). The embryo shown in A and B is the same as that in Fig. 10A,B. (C-F) During undifferentiated blastodermal stages (C,D), *Tc-mael* is expressed in a distinct posterior expression domain (arrow) that is maintained in differentiated blastodermal stages and invagination (E,F).

Table 1. Official gene set number (Tc), iBeetle (iB) number (http://ibeetle-base.uni-goettingen.de), *Drosophila* ortholog, molecular function and changes in relative expression of candidate genes

Tc number	iB number	*Dm* ortholog	Molecular function	Relative expression *tsl* RNAi	*cic* RNAi
TC004989	iB_00793	cathD	Aspartic-type endopeptidase activity	↓	↑
TC006235	iB_04097	Dsp1	DNA binding, bending; transcription factor binding	↓	↑
TC009922	-	ap2	Protein transporter activity	↓	↑
TC004241	iB_03713	-	Hydroxylase function	↑	↑
TC006282	-	Geminin	DNA binding	↓	↑
TC006181	iB_01008	CG43129	Unknown	↓	↑
TC008122	iB_04429	CG8408	Unknown	↓	↑
TC005697	iB_00909	CG9323	RNA helicase activity, G-quadruplex RNA binding	↓	↑
TC003946	iB_00642	crol	Metal ion binding; nucleic acid binding	↓	↑
TC000868	iB_03094	elB	Metal ion binding; nucleic acid binding; protein binding	↓	↑
TC007740	iB_04375	-	Unknown	↑	-
TC013474	-	Sens	Transcription factor activity, sequence-specific DNA binding	↓	↑

Candidate genes were sorted according to Fig. 4. -, not assigned.

elongation, but also results in deformation of the larval head (Fig. 4). For two genes (*TC004241* and *TC008122*), we observed the loss of the entire head without obvious axis elongation phenotypes (Fig. 4). These head phenotypes resemble that of mild *Tc-cic* RNAi (Figs 1 and 4) and thus may represent gain-of-function phenotypes of the terminal system.

Although it remains to be elucidated the degree to which these candidate genes are indeed direct target genes of Torso signalling, our study establishes that transcriptome sequencing facilitates the identification of novel candidate genes for early anterior and posterior pattern formation in *Tribolium*.

### Tribolium *Maelstrom* RNAi results in the loss of growth-zone derived structures

We selected the *Tribolium* ortholog of *the Drosophila maelstrom* gene for closer inspection. Maelstrom (Mael) is a conserved PIWI-interacting RNA factor (piRNA), consisting of two domains: a HMG box and a MAEL domain (Sato and Siomi, 2015). In *Drosophila*, piRNA factors are required for transcriptional transposon silencing in both germ and ovarian somatic cells (Sato and Siomi, 2015). In addition, Mael coordinates axis specification through nucleating microtubule-organizing centre (MTOC) components (Sato et al., 2011).

The *Tribolium* genome contains a single *maelstrom* ortholog (*Tc-mael*, *TC008172*). *Tc-mael* is expressed maternally and transcripts accumulate at the anterior pole of unfertilized eggs and the polar body (Fig. 5A). During blastoderm stages, *Tc-mael* becomes expressed at the posterior pole. This domain persists until gastrulation (Fig. 5C,E). Later, *Tc-mael* expression is no longer detectable (not shown).

Knocking down *Tc-mael* by RNAi results in truncation phenotypes (Fig. 6 and Fig. S2). About 60% of the larvae lack growth-zone derived structures: abdominal segments and terminal structures are lost, resembling the loss of Torso signalling (Schoppmeier and Schröder, 2005). These posterior truncation phenotypes were sometimes (about 20%) accompanied by aberrations of the larval head, likely representing stronger phenotypes. Head phenotypes, however, are highly variable and may include deformations and/or deletions of pre-gnathal and gnathal segments. Although phenotypes likely reveal hat *Tribolium mael* functions in early embryonic patterning (see below), we observed additional effects of *Tc-mael* depletion. RNAi with *Tc-mael* results in incorrect dorsal closure, generating completely or partially everted ('inside-out') larvae (12.5%). These larvae may have escaped the primary truncation effect.

To analyse the impact of *Tc-mael* RNAi, we performed time-lapse recordings of EFA-nGFP embryos (Fig. 7 and Movie 3) (Sarrazin et al., 2012). Upon *Tc-mael* RNAi, anterior germ-rudiment formation is impaired: head anlagen of *Tc-mael* RNAi embryos are less condensed than wild type (Fig. 7E). During wild-type germ-band elongation, the head region extends to an anterior-dorsal position and the germ-band extends posteriorly (Fig. 7 and Movie 1). Upon *Tc-mael* RNAi, the head anlagen still moves in anterior ventral direction; posterior invagination, however, is delayed to some degree (Fig. 7D and Movie 3) and elongation fails (Fig. 7J,K,L; and Movie 3), supporting a function for *Tc-mael* in growth-zone formation and/or axis elongation (see below).

In *Tc-mael* RNAi embryos, the serosal window eventually closes and amniotic cavity formation seems normal (Fig. 7E,F; Movie 3). Unexpectedly, we observed the premature rupturing of the serosa at a
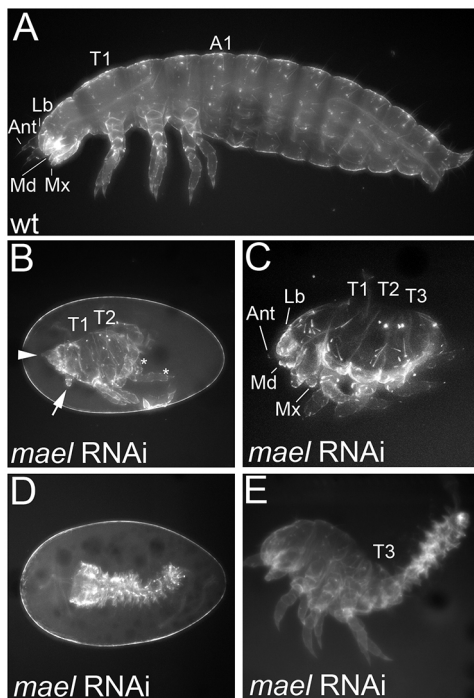
Fig. 6. *Tc-mael* RNAi. (A-D) Cuticle of wild-type (A) and *Tc-mael* RNAi (B-D) larvae. (B) Only remnants of pre-gnathal and gnathal segments are left (arrows). The third thoracic segment is still formed (asterisks), but all abdominal segments are deleted. (C) Weaker phenotypes show the reduction of the head capsule. All abdominal segments are deleted. (D,E) *Tc-mael*-RNAi also results in inside-out phenotypes that affect the whole larva (D) or only posterior segments (E).
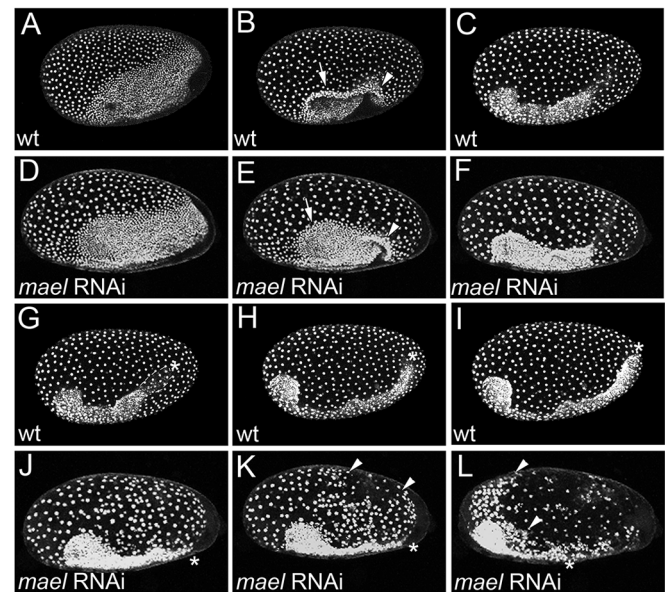
Fig. 7. Live imaging of *Tc-meal* RNAi. Live imaging detection of wild-type (A,B,G,H) and *Tc-cic* RNAi (D-F,J-L) in the transgenic *Tribolium* EFA-nGFP line. Columns show nGFP-labelled stage-matched embryo at representative time-points. (A-C) In wild type, the embryonic anlagen gives rise to germ rudiment that becomes covered by the serosa (B, arrowhead and arrow). (D-F) Upon *Tc-mael* RNAi, head anlagen are expanded and less condensed (E, arrow). In addition, the rim of the serosa window is initially less condensed (E, arrow and arrowhead). In wild type, the germ-band extends posteriorly (G-I, asterisks). In *Tc-mael* RNAi, posterior elongation fails (J-L, asterisks). In addition, the serosa ruptures prematurely (K,L, arrowheads).

posterior-dorsal position (Fig. 7K,L; Movie 3). In wild type, serosal withdrawal does not occur until the onset of dorsal closure at an anterior-ventral position (Hilbrant et al., 2016; Panfilio et al., 2013).

Rupture of extra-embryonic membranes is a coordinated process that involves opening both the serosa and the amnion in an anterior-ventral region, after germ-band retraction (Hilbrant et al., 2016; Panfilio et al., 2013). If the amnion fails to withdraw prior to embryonic dorsal closure, the embryo becomes everted ('inside-out') (Hilbrant et al., 2016; Panfilio et al., 2013). Proper serosal patterning (and subsequent withdrawal) involves the attachment of the serosa to the vitelline membrane at the posterior pole of the egg (Koelzer et al., 2014). In *Tc-mael* RNAi, however, the posterior serosa never seems to come into contact with the vitelline membrane at the posterior egg pole, but rather contracts anteriorly, loses tissue integrity and ultimately disintegrates (Fig. 7J-L, Movie 3).

Fig. 8. Expression of *Tc-zen-1*, *Tc-eve* and *Tc-gt* in *Tc-mael* RNAi. Embryos double-stained for *Tc-eve* and *Tc-zen-1* (A-H) and *Tc-gt* (I,J). Embryos in C,D,G were subsequently stained with Hoechst 33342 (E,F,H). In *Tc-mael* RNAi, the serosa anlagen is reduced (B, arrowheads). The first and second primary *Tc-eve* domains (B, bars) are present (C,E). In wild type, *Tc-zen-1* is expressed at the margin of the serosa window. (D,F) In *Tc-mael* knockdown, *Tc-zen-1* expression lost from the anterior rim of serosa window (D, arrow). The head primordia is less condensed (D, arrow; F, asterisks). (G) The fourth primary *Tc-eve* domain does not form properly and, in addition, posterior morphology eventually becomes highly irregular. (I) In wild-type blastoderm embryos, *Tc-gt* is expressed in a head domain (bars) and at the posterior pit (asterisk). (J) The posterior *Tc-gt* domain is lost in *Tc-mael RNAi* (asterisk), while the head domain (bars) is still present.

Consequently, the embryo is stuck inside the amniotic tissue and the embryo closes ventrally rather than dorsally, resulting in inside-out phenotypes.

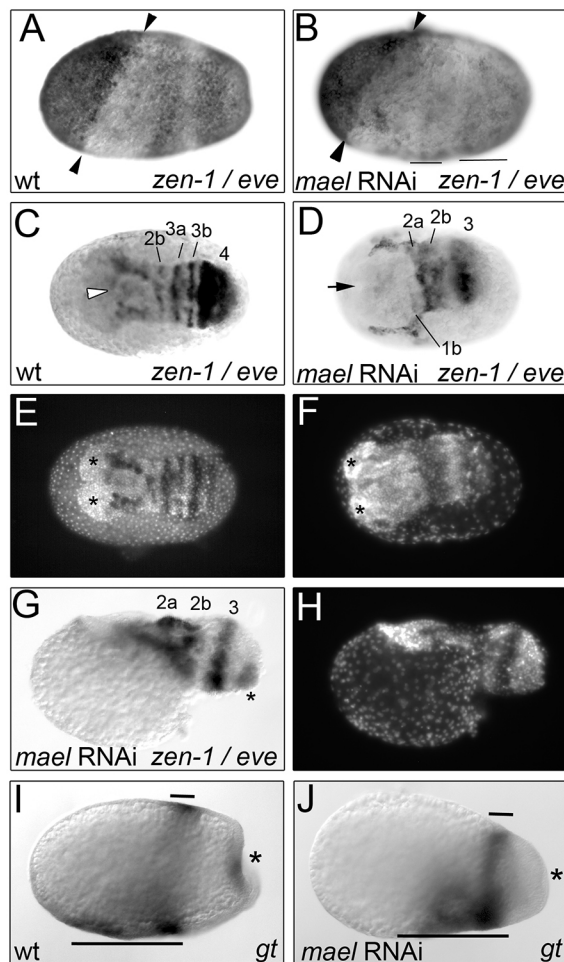## Maelstrom affects anterior patterning and morphogenesis

To uncover the influence of *Tc-mael* on the formation of extra-embryonic membranes and patterning of anterior embryonic anlagen in more detail, we visualized the emergence of these primordia by analysing the *Tc-eve*, *Tc-giant* (*Tc-gt*), and *Tc-zen-1* expression (Falciani et al., 1996; Patel et al., 1994) (Fig. 8). Upon *Tc-mael* knockdown, the *Tc-zen-1* domain is smaller, indicating a reduction of the serosa primordia (Fig. 9B). However, the serosa-germ-rudiment border is still oblique.

In wild-type differentiated blastoderm stage, *Tc-gt* is expressed in a wedge-shaped anterior domain comprising pre-gnathal and gnathal segments (Bucher and Klingler, 2004). At that stage a secondary domain also arises at the posterior pole (Bucher and Klingler, 2004). In *Tc-mael* RNAi, the anterior domain is unaffected, whereas the posterior *Tc-gt* domain is lost (see below). In addition, the first and second primary *Tc-eve* domains (*Tc-eve* stripe 1 and stripe 2) are present in blastoderm stages, but reduced and less defined to some degree (Fig. 8B,D).
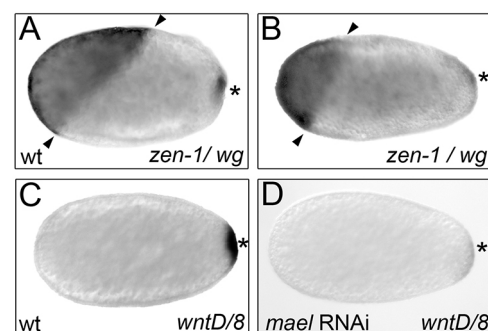
During gastrulation, extra-embryonic membranes fold over anterior and posterior embryonic margins, thereby completing the rim of a serosal window (Handel et al., 2000). *Tc-zen-1* is expressed throughout serosal window formation and closure, with high expression levels at the margin of the serosa window (Fig. 8C). Upon *Tc-mael* knockdown, *Tc-zen-1* expression is lost from the anterior rim of serosa window (Fig. 8D,G) and head primordia appear to be less condensed and are shifted towards the anterior pole of the egg (Fig. 8D). At that stage there are no obvious effects on anterior *Tc-eve* expression. The first and second primary *Tc-eve* stripes have split, while the 3rd double-segmental domain is present (Fig. 9G), reflecting that gnathal and thoracic anlagen are present. Thus, *Tc-mael* is required for proper serosal size regulation and head morphogenesis.

Maelstrom is required for axis elongation and growth-zone formation

Tc-mael RNAi embryos are depleted of abdominal segments (Figs 7 and 8). The fourth primary *Tc-eve* domain, which corresponds to

Fig. 9. Expression of Wnt genes in *Tc-mael* RNAi. Expression of *Tc-wg* (A,B) and *Tc-wntD/8* (C,D) in wild type (A,C) and *Tc-mael* RNAi (B,D) embryos. Embryos in B,D were subsequently stained with Hoechst 33342. Embryos in A, B were double stained for *Tc-zen1*. (A) In wild-type undifferentiated blastoderm, *Tc-zen-1* covers the anlagen of the serosa (arrowheads) and *Tc-wg* is expressed at the posterior pole (asterisk). (B) In *Tc-mael* RNAi, the *Tc-zen-1* expression domain is reduced (arrowheads), while posterior *Tc-wg* expression is still present (asterisk). (C) *Tc-wntD/8* is expressed at the posterior pole (asterisk). (D) Upon *Tc-mael* RNAi, this domain is notably reduced (asterisk) or even absent.

the first and second abdominal segments, does not form properly and, in addition, posterior morphology becomes highly irregular (Fig. 8G,H). Already during late differentiated blastoderm stages, the posterior *Tc-gt* domain is lost (Fig. 8J), indicating that posterior elongation is already affected at that stage.

To reveal whether *Tc-mael* is already involved in setting up a functional growth zone, we monitored the expression of *Tc-wg* and *Tc-wntD/8* (Bolognesi et al., 2008a,b) (Fig. 9). In wild type, Wnt signalling is required for growth-zone formation and axis elongation (Beermann et al., 2011; Bolognesi et al., 2008a,b). Although in *Tc-mael* RNAi the terminal *Tc-wg* domain was basically present, the *wntD/8* is notably reduced or even absent (Fig. 9C), resembling the situation in *Tc-tor* or *Tc-tsl* knockdown. Our results indicate that posterior patterning by Torso may be realized through *Tc-maelstrom*-dependent activation of the posterior *Tc-wntD/8* domain.

Next, we monitored *Tc-mael* expression in both *Tc-tsl*- and *Tc-cic*-depleted embryos. As expected, we observed an expansion of *Tc-mael* expression in *Tc-cic* RNAi (Fig. 10E), whereas in *Tc-tsl* RNAi expression was lost (Fig. 10C). Thus, *Tribolium* Maelstrom is indeed a target gene of the terminal system in this beetle.
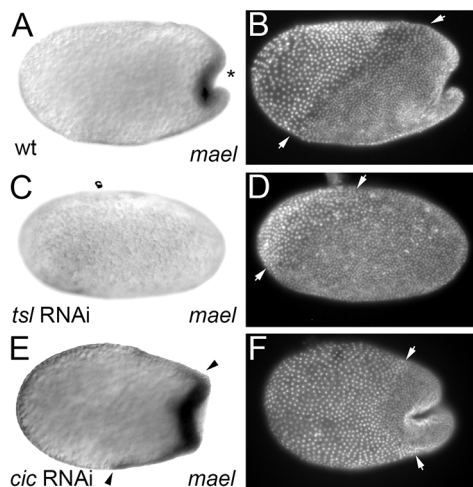
Posterior retraction of short-gastrulation depends on Maelstrom activity

Given that *Drosophila maelstrom* is also required for achieving proper DV polarity (Clegg et al., 2001, 1997; Findley et al., 2003; Sato et al., 2011), we monitored DV axis formation upon *Tc-mael* RNAi. It has been shown before that the dorsoventral tilt of the serosa/embryo boundary depends on BMP signalling in *Tribolium* (Nunes da Fonseca et al., 2008; van der Zee et al., 2006). In *Tc-dpp* RNAi, this border becomes DV symmetric and is shifted towards the anterior. Depletion *Tc-sog* has opposing effects. The serosa increases at the expense of the head anlagen and the serosa-embryo boundary develops vertical to the egg axis (van der Zee et al., 2006). Thus, the loss of DV asymmetry reveals impaired dorsoventral (DV) patterning in *Tribolium* (van der Zee et al., 2006).
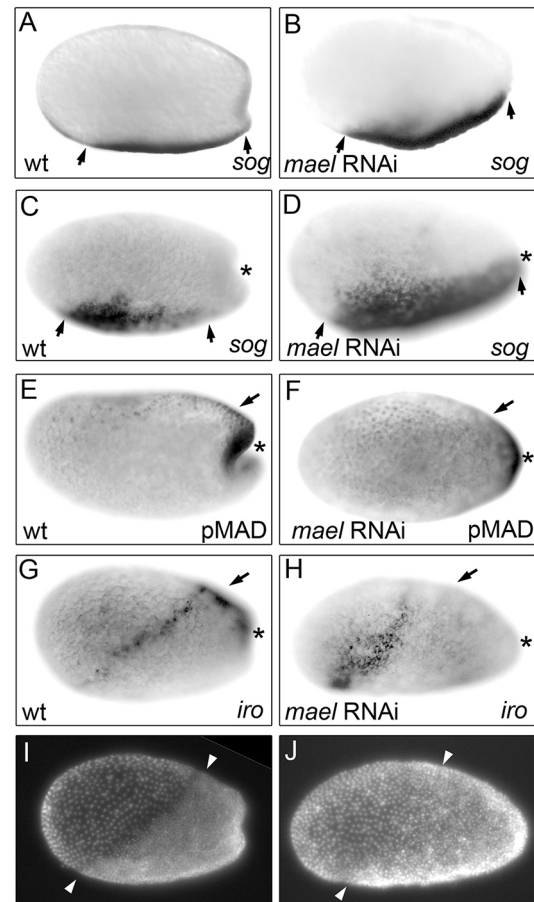
Although also in *Tc-mael* RNAi the serosal anlagen are reduced (Fig. 8B), the serosa-germ-rudiment border is still oblique (Fig. 8B), indicating that DV axis formation is unaffected. This is corroborated

by anterior *Tc-gt* expression (Fig. 8J). In *Tc-mael* RNAi, the *gt* domain still shows a pronounced DV asymmetry. Thus, *Tc-mael* has no impact of on early anterior DV axis polarization.

Interestingly, however, we found *Tc-mael* to be required for posterior *Tc-sog* retraction (Fig. 11). In wild type, *Tc-sog* is initially expressed in a broad ventral domain, which subsequently clears from the posterior pole (van der Zee et al., 2006) (Fig. 11A,C). Although there is no pronounced difference in early stages, *Tc-sog* fails to retract from the posterior pole of *Tc-mael* RNAi embryos (Fig. 11D) and posterior dorsal Dpp activity (as monitored by pMAD staining) (Fig. 11F) is reduced to some degree. Consequently, posterior dorsal tissue (i.e. the dorsal amnion) lacks peak levels of Dpp activity. In wild type, *Tc-iro* is expressed in a domain marking the anterior border of the germ rudiment, which will give rise to the anterior amnion. In addition, *Tc-iro* is expressed

Fig. 11. *Tc-mael* RNAi in dorsoventral patterning. Wild-type (A,C,E,G,I) and *Tc-mael* RNAi (B,D,F,H,J) embryos stained for *Tc-sog* (A-D), pMAD (E,F) and *Tc-iro* (G,H). Embryos in G,H were subsequently stained with Hoechst 33342 (I,J). In wild-type blastoderm (A), *Tc-sog* is expressed in a broad ventral domain (arrows), which (C) eventually retracts from the posterior pole (asterisk). Upon *Tc-mael* RNAi, the (B) early *Tc-sog* domain might be somewhat stronger (arrows), otherwise there is no pronounced difference. (D) Later, *Tc-sog* fails to retract from the posterior pole (asterisk). (E) Wild-type Dpp activity (as monitored by pMAD staining) peaks in the posterior dorsal region of the embryo (arrow and asterisk). (F) In *Tc-mael* RNAi, posterior pMAD signal is still present (asterisk), while dorsal Dpp activity seems to be reduced (arrow). In wild type (G,I), *Tc-iro* is expressed in the anterior and dorsal (arrow) amnion that expands towards the posterior pole (asterisk). (H,J) In *Tc-mael* RNAi embryos, anterior *Tc-iro* expression is maintained and still oblique. The posterior dorsal expression domain is absent (arrow and asterisk). Arrowheads in I,J indicate the serosa/embryo boundary.

Fig. 10. *Tc-mael* is a target gene of the terminal system. Expression of *Tc-mael* in wild type (A), *Tc-tsl* RNAi (C) and *Tc-cic* RNAi (E) embryos. Embryos in A,C,E were subsequently stained with Hoechst 33342 (B,D,F). The embryo shown A and B is the same as that in Fig. 5A,B. (C) In *Tc-tsl* RNAi, *Tc-mael* expression is lost, while the *Tc-mael* domain expands upon *Tc-cic* RNAi (E). Arrowheads indicate the serosa/embryo boundary.

in the dorsal amnion (Nunes da Fonseca et al., 2008). In *Tc-mael* RNAi embryos, the anterior of *Tc-iro* expression was maintained, whereas the dorsal most expression domain was absent (Fig. 11H). Thus, in *Tc-mael* RNAi embryos, posterior dorsal tissue is lateralized.

DISCUSSION
The function of *Tribolium capicua* is restricted to AP patterning
The depletion of *Tribolium capicua* results in the expansion of terminal anlagen and de-repression of terminal target genes, reflecting de-repression (i.e. gain of function) phenotypes of Torso signalling. This resembles the situation in *Drosophila* (Jimenez et al., 2000; Paroush et al., 1997), indicating that Torso signalling induces gene expression by also relieving Cic-mediated repression in *Tribolium*.

Although the functions of *Tribolium capicua* in terminal patterning may very well be conserved, we did not observe any obvious impact of *Tc-cic* on dorsoventral pattern formation. In *Drosophila*, the function of Cic is not restricted to Torso-RTK signalling. During *Drosophila* oogenesis, Cic is required to translate EGFR signalling into asymmetric *pipe* expression, which culminates in the establishment of a nuclear Dorsal gradient (Moussian and Roth, 2005).

In *Tribolium*, EGF signalling has broadly conserved roles in setting up the DV axis of the embryo (Lynch et al., 2010). The depletion of the *Tribolium gurken* ortholog (*Tc-Tgf-alpha*) results in the ventralization of embryos, resembling *Tc-dpp* RNAi phenotypes to some degree (van der Zee et al., 2006). In both *Tc-Tgf-α* and *Tc-dpp RNAi*, the first morphologically visible sign of DV polarity, the obliqueness of the border between serosa and germ rudiment, is lost (Lynch et al., 2010; van der Zee et al., 2006). However, as indicated by morphology and *Tc-zen-1* expression, *Tc-cic* RNAi does not affect the obliqueness of the serosa/germ-rudiment border (Figs 2 and 3). Thus, in *Tribolium* there is no obvious antagonistic interaction of EGFR signalling with Cic in embryonic DV axis formation.

The expansion of the serosa in *Tc-cic* RNAi embryos goes along with de-repression of *Tc-zen-1* (Fig. 3G,I). At first glance this situation resembles that of *Drosophila*, as knockdown of *Dm-cic* results in the lateral expansion of *Dm-zen* expression (Astigarraga et al., 2007; Jimenez et al., 2000; Kim et al., 2011). In *Drosophila*, *zen* is broadly activated by maternal factors (Rushlow et al., 1987). During early blastoderm stages, *cic* participates in the ventral and lateral repression of *zen* by Dorsal (Dl) (Astigarraga et al., 2007; Jimenez et al., 2000; Kim et al., 2011). At the poles, Dl-mediated repression of *zen* is antagonized by Torso signalling (Rusch and Levine, 1994), which likely depends on MAPK-dependent downregulation of Cic (Kim et al., 2011). However, the situation in *Tribolium* differs from *Drosophila*. The distinction between serosa and germ rudiment is primarily set up by inputs from the AP system and secondarily modulated through DV signalling. In particular, *Tc-zen-1* expression and, thus, serosa size regulation depend on the combined activity of terminal signalling and *Tc-orthodenticle* (Kotkamp et al., 2010), whereas the obliqueness of the border between serosa and germ-rudiment is subsequently established by EFGR and BMP signalling (Lynch et al., 2010; Nunes da Fonseca et al., 2010, 2008; van der Zee et al., 2008, 2006). Given that serosal size regulation, but not the obliqueness of the border between serosa and germ rudiment is affected in *Tc-cic* RNAi, it appears that eggs produced after *Tc-cic* depletion maintain normal embryonic DV polarity.

Maelstrom is required for serosa morphogenesis and anterior germ-band condensation
The depletion of *Tribolium maelstrom* by RNAi affects axis elongation, germ-band condensation and the formation of the extra-embryonic serosa (Figs 6–8). In *Drosophila*, Mael coordinates oocyte polarity through interaction with components of the MTOC (Sato et al., 2011). Achieving proper cell polarity is essential for diverse processes, including cell shape changes and cell migration, asymmetric cell division, and morphogenesis (St Johnston and Ahringer, 2010). In addition, early *Tribolium* development depends on extensive cell-polarization events (Benton et al., 2013; Handel et al., 2000). RNAi with *Tc-mael* disturbs the anterior condensation of the embryonic anlagen (Figs 7 and 8). Hence, in absence of *Tc-mael*, cell polarity may not be established appropriately, which in turn may affect early morphogenesis. This would be equivalent to the situation in *Drosophila* (Clegg et al., 2001, 1997; Findley et al., 2003; Sato et al., 2011). Although we currently cannot exclude the possibility that *Tc-mael* RNAi phenotypes are due to impaired transposon silencing, we posit that *Tc*-Mael coordinates cell polarity (possibly by acting on MTOC organization) at least in serosa morphogenesis and anterior germ-band condensation in a Torso signalling-dependent manner.

Although serosa phenotypes indeed resemble aspects of *Tc-tsl* or *Tc-tor* RNAi phenotypes, we observed additional defects in head development upon *Tc-mael* knockdown. At first glance *Tc-mael* RNAi head phenotypes are not related to terminal patterning. As mentioned before, anterior Torso-signalling is involved in serosal size regulation (Schoppmeier and Schröder, 2005). The loss or reduction of this extra-embryonic membrane by *Tc-tsl* or *Tc-zen-1* RNAi results in the expansion of the head anlagen, which is largely compensated for later in development (Schoppmeier and Schröder, 2005; van der Zee et al., 2005). Nevertheless, a small faction of larvae depleted for *Tc-zen-1* or *Tc-tsl* do also display head defects (van der Zee et al., 2005) (F.P. and M.S., unpublished). These phenotypes are highly variable and, thus, may instead reflect defects during size compensation and head morphogenesis rather than specific functions in head patterning.

Tribolium maelstrom in posterior patterning
At the posterior pole, *Tc-mael* function is necessary for growth-zone formation. Upon *Tc-mael* knockdown, expression of *Tc-wntD/8* is lost and posterior elongation is terminated prematurely (Figs 6 and 9). Given that *Tc-wntD/8* is under the control of Torso signalling (Fig. 3) (Bolognesi et al., 2008b; Schoppmeier and Schröder, 2005), our results suggest that posterior patterning by Torso may be realized, at least in part, through Maelstrom-dependent activation or positioning of posterior Wnt domains.

On the other hand, the knock-down of *Tc-wntD/8* only results in a small percentage of embryos lacking abdominal segments and additional removal of *Tc-wg* only enhanced the penetrance of this phenotype to some degree (Bolognesi et al., 2008a). As the effects of *Tc-mael* RNAi on growth-zone formation and axis elongation are considerably more severe, *Tc-mael* likely fulfils additional functions in posterior patterning, which may involve DV patterning.

In *Tc-mael* RNAi embryos, posterior *Tc-sog* expression fails to retract and, as a consequence, posterior dorsal tissue, i.e. the dorsal amnion, lacks peak levels of Dpp activity. Changes in Dpp activity also affect morphogenetic movements during gastrulation (Nunes da Fonseca et al., 2010; van der Zee et al., 2006). Upon *Tc-dpp* RNAi, for example, the germ-band is symmetrically folded inwards at the posterior pit and extends toward the anterior. In *Tc-mael*

RNAi embryos, however, we did not observe any strong effects on posterior invagination, and posterior amniotic fold formation is normal, suggesting that posterior morphogenetic movements might be largely unaffected. Thus, even though *Tc-mael* also contributes – in a Torso-independent manner – to proper DV axis formation, we deem it unlikely that this function has an impact on early posterior axis polarization or growth-zone formation.

During oogenesis, *Drosophila mael* mutants fail to establish cytoplasmic polarity and to accumulate Gurken normally. In addition, other polarity markers (e.g. *osk, BicD*) fail to accumulate in the posterior ooplasm, and *bcd* mRNA becomes localized at both poles (Clegg et al., 2001, 1997; Findley et al., 2003; Sato et al., 2011). The *Tribolium grk* ortholog has no major role in AP axis formation, but rather acts in DV patterning (Lynch et al., 2010). Moreover, *Tc-wntD/8* is not maternally expressed, indicating that additional potentially localized factors might be involved in wntD/8 regulation.

An important role for localized maternal determinants has long been postulated for several insect taxa, including crickets, beetles and flies. However, thus far, the existence of two morphogenetic centres (anterior and posterior) has been proven only for the long-germ wasp *Nasonia vitripennis* (Rosenberg et al., 2009). *Tribolium* uses anterior mRNA localization to some degree (Fu et al., 2012). Posterior localized maternal determinants, however, have not yet been identified (Schmitt-Engel et al., 2012). Although posterior patterning in *Tribolium* may depend on spatially restricted polarity cues (i.e. the terminal system) that regulate short-range acting target genes required for axis elongation, such as Wnt signalling (Beermann et al., 2011; Bolognesi et al., 2008a,b), rather than on long-range acting gradients (i.e. Nanos) (Schmitt-Engel et al., 2012), it is tempting to speculate that *Tc-mael* promotes growth-zone formation by localizing an as yet unknown posterior maternal determinant.

MATERIALS AND METHODS
Histology
Fixation and single *in situ* and immunofluorescence staining were performed using standard protocols (Patel et al., 1989; Tautz and Pfeifle, 1989). Embryos were subsequently counterstained with Hoechst 33342.

RNAi
Parental RNAi and dsRNA synthesis was performed as described previously (Bucher and Klingler, 2004; Bucher et al., 2002). dsRNAs were injected into female pupae at a concentration of 1 μg/μl. RNAi phenotypes were confirmed by injection of non-overlapping-dsRNA fragments. RNAi for all fragments resulted in identical phenotypes, excluding the possibility that an unrelated gene was affected (off-target effects).

Cuticle preparation
First instar larvae were cleared in lactic acid/10% ethanol overnight at 60°C. Cuticles were transferred to a drop of lactic acid on a slide. The cuticular autofluorescence was detected on a Zeiss Axiophot microscope, and maximum projection images were created from *z* stacks using the Analysis D software (Olympus).

Transcriptome sequencing
Sequencing was carried out on a SOLiD 4 system (Life Technologies) using 50 bp fragment reads. Mapping to the Tcas3 reference genome (http://bioinf.uni-greifswald.de/gb2/gbrowse/tribolium/) and counting were performed using LifeScope version 2.5 (Life Technologies). In order to filter out adapters, ribosomal and tRNAs, a filter reference file was created using the adapter sequences provided by Life Technologies, large and small subunit rRNA sequences from the reference, and the results of a tRNAscan-SE (v1.1) run over the reference sequence.

Samples T1 (wild type), T2 (*tsl* RNAi) and T3 (*cic* RNAi) mapped read counts were 15,517,184; 6,172,710 and 31,441,775, respectively. Counting yielded read counts for 143,603 exons in 16,543 transcripts, as provided by the Tcas3 reference. Normalization and comparison of expression levels between all three samples was performed using the differential expression analysis for sequence count data algorithm (DESeq) (Anders and Huber, 2010).

Live imaging
For time-lapse imaging, the EFA-nGFP-strain of *Tribolium castaneum* was used (Sarrazin et al., 2012). Embryos (4-6 h) were treated with 12.5% bleach twice for 30 s and then rinsed with tap water. Embryos were then mounted in a hanging drop of Sigma Halocarbon oil 700.

For time-lapse imaging, a Leica TCS SP5 II Confocal System was used. Stacks were recorded about every 12 min for an interval of 12 h at 10× magnification at 20°C. Processing of the image stacks was carried out in LAS AF Version 2.4.1 build 638 and Fiji (Schindelin et al., 2012).

Data availability
The complete dataset, including all relevant parameters, has been deposited with NCBI under BioProject PRJNA311251.

Supplementary information
Supplementary information available online at
http://dev.biologists.org/lookup/doi/10.1242/dev.136853.supplemental

References
Ajuria, L., Nieva, C., Winkler, C., Kuo, D., Samper, N., Andreu, M. J., Helman, A., Gonzalez-Crespo, S., Paroush, Z., Courey, A. J. et al. (2011). Capicua DNA-binding sites are general response elements for RTK signaling in Drosophila. *Development* **138**, 915-924.

Anders, S. and Huber, W. (2010). Differential expression analysis for sequence count data. *Genome Biol.* **11**, R106.

Astigarraga, S., Grossman, R., Díaz-Delfínn, J., Caelles, C., Paroush, Z. and Jiménez, G. (2007). A MAPK docking site is critical for downregulation of Capicua by Torso and EGFR RTK signaling. *EMBO J.* **26**, 668-677.

Barker, D. D., Wang, C., Moore, J., Dickinson, L. K. and Lehmann, R. (1992). Pumilio is essential for function but not for distribution of the Drosophila abdominal determinant Nanos. *Genes Dev.* **6**, 2312-2326.

Beermann, A., Pruhs, R., Lutz, R. and Schroder, R. (2011). A context-dependent combination of Wnt receptors controls axis elongation and leg development in a short germ insect. *Development* **138**, 2793-2805.

Benton, M. A., Akam, M. and Pavlopoulos, A. (2013). Cell and tissue dynamics during Tribolium embryogenesis revealed by versatile fluorescence labeling approaches. *Development* **140**, 3210-3220.

Bolognesi, R., Beermann, A., Farzana, L., Wittkopp, N., Lutz, R., Balavoine, G., Brown, S. J. and Schröder, R. (2008a). Tribolium Wnts: evidence for a larger repertoire in insects with overlapping expression patterns that suggest multiple redundant functions in embryogenesis. *Dev. Genes Evol.* **218**, 193-202.

Bolognesi, R., Farzana, L., Fischer, T. D. and Brown, S. J. (2008b). Multiple Wnt genes are required for segmentation in the short-germ embryo of Tribolium castaneum. *Curr. Biol.* **18**, 1624-1629.

Bucher, G. and Klingler, M. (2004). Divergent segmentation mechanism in the short germ insect Tribolium revealed by giant expression and function. *Development* **131**, 1729-1740.

Bucher, G., Scholten, J. and Klingler, M. (2002). Parental RNAi in Tribolium (Coleoptera). *Curr. Biol.* **12**, R85-R86.

Casanova, J. (2005). Developmental evolution: torso–a story with different ends? *Curr. Biol.* **15**, R968-R970.

Clegg, N. J., Frost, D. M., Larkin, M. K., Subrahmanyan, L., Bryant, Z. and Ruohola-Baker, H. (1997). maelstrom is required for an early step in the establishment of Drosophila oocyte polarity: posterior localization of grk mRNA. *Development* **124**, 4661-4671.

Clegg, N. J., Findley, S. D., Mahowald, A. P. and Ruohola-Baker, H. (2001). Maelstrom is required to position the MTOC in stage 2-6 Drosophila oocytes. *Dev. Genes Evol.* **211**, 44-48.

de las Heras, J. M. and Casanova, J. (2006). Spatially distinct downregulation of Capicua repression and tailless activation by the Torso RTK pathway in the Drosophila embryo. *Mech. Dev.* **123**, 481-486.

Driever, W. and Nüsslein-Volhard, C. (1988). The bicoid protein determines position in the Drosophila embryo in a concentration-dependent manner. *Cell* **54**, 95-104.

Falciani, F., Hausdorf, B., Schroder, R., Akam, M., Tautz, D., Denell, R. and Brown, S. (1996). Class 3 Hox genes in insects and the origin of zen. *Proc. Natl. Acad. Sci. USA* **93**, 8479-8484.

Findley, S. D., Tamanaha, M., Clegg, N. J. and Ruohola-Baker, H. (2003). Maelstrom, a Drosophila spindle-class gene, encodes a protein that colocalizes with Vasa and RDE1/AGO1 homolog, Aubergine, in nuage. *Development* **130**, 859-871.

Fu, J., Posnien, N., Bolognesi, R., Fischer, T. D., Rayl, P., Oberhofer, G., Kitzmann, P., Brown, S. J. and Bucher, G. (2012). Asymmetrically expressed axin required for anterior development in Tribolium. *Proc. Natl. Acad. Sci. USA* **109**, 7782-7786.

Furriols, M. and Casanova, J. (2003). In and out of Torso RTK signalling. *EMBO J.* **22**, 1947-1952.

Grillo, M., Furriols, M., de Miguel, C., Franch-Marro, X. and Casanova, J. (2012). Conserved and divergent elements in Torso RTK activation in Drosophila development. *Sci. Rep.* **2**, 762.

Handel, K., Grünfelder, C. G., Roth, S. and Sander, K. (2000). Tribolium embryogenesis: a SEM study of cell shapes and movements from blastoderm to serosal closure. *Dev. Genes Evol.* **210**, 167-179.

Hilbrant, M., Horn, T., Koelzer, S. and Panfilio, K. A. (2016). The beetle amnion and serosa functionally interact as apposed epithelia. *eLife* **5**, e13834.

Jimenez, G., Guichet, A., Ephrussi, A. and Casanova, J. (2000). Relief of gene repression by torso RTK signaling: role of capicua in Drosophila terminal and dorsoventral patterning. *Genes Dev.* **14**, 224-231.

Johnson, T. K., Henstridge, M. A., Herr, A., Moore, K. A., Whisstock, J. C. and Warr, C. G. (2015). Torso-like mediates extracellular accumulation of Furin-cleaved Trunk to pattern the Drosophila embryo termini. *Nat. Commun.* **6**, 8759.

Kim, Y., Andreu, M. J., Lim, B., Chung, K., Terayama, M., Jiménez, G., Berg, C. A., Lu, H. and Shvartsman, S. Y. (2011). Gene regulation by MAPK substrate competition. *Dev. Cell* **20**, 880-887.

Klingler, M. (2004). Tribolium. *Curr. Biol.* **14**, R639-R640.

Koelzer, S., Kölsch, Y. and Panfilio, K. A. (2014). Visualizing late insect embryogenesis: extraembryonic and mesodermal enhancer trap expression in the beetle Tribolium castaneum. *PLoS ONE* **9**, e103967.

Kotkamp, K., Klingler, M. and Schoppmeier, M. (2010). Apparent role of Tribolium orthodenticle in anteroposterior blastoderm patterning largely reflects novel functions in dorsoventral axis formation and cell survival. *Development* **137**, 1853-1862.

Li, W. X. (2005). Functions and mechanisms of receptor tyrosine kinase Torso signaling: lessons from Drosophila embryonic terminal development. *Dev. Dyn.* **232**, 656-672.

Liaw, G.-J. and Lengyel, J. A. (1993). Control of tailless expression by bicoid, dorsal and synergistically interacting terminal system regulatory elements. *Mech. Dev.* **40**, 47-61.

Lynch, J. A., Peel, A. D., Drechsler, A., Averof, M. and Roth, S. (2010). EGF signaling and the origin of axial polarity among the insects. *Curr. Biol.* **20**, 1042-1047.

Macdonald, P. M. (1992). The Drosophila pumilio gene: an unusually long transcription unit and an unusual protein. *Development* **114**, 221-232.

Mineo, A., Furriols, M. and Casanova, J. (2015). Accumulation of the Drosophila Torso-like protein at the blastoderm plasma membrane suggests that it translocates from the eggshell. *Development* **142**, 1299-1304.

Moussian, B. and Roth, S. (2005). Dorsoventral axis formation in the Drosophila embryo–shaping and transducing a morphogen gradient. *Curr. Biol.* **15**, R887-R899.

Nagy, L. M. and Carroll, S. (1994). Conservation of wingless patterning functions in the short-germ embryos of Tribolium castaneum. *Nature* **367**, 460-463.

Nunes da Fonseca, R., von Levetzow, C., Kalscheuer, P., Basal, A., van der Zee, M. and Roth, S. (2008). Self-regulatory circuits in dorsoventral axis formation of the short-germ beetle Tribolium castaneum. *Dev. Cell* **14**, 605-615.

Nunes da Fonseca, R., van der Zee, M. and Roth, S. (2010). Evolution of extracellular Dpp modulators in insects: the roles of tolloid and twisted-gastrulation in dorsoventral patterning of the Tribolium embryo. *Dev. Biol.* **345**, 80-93.

Nüsslein-Volhard, C., Frohnhofer, H. G. and Lehmann, R. (1987). Determination of anteroposterior polarity in Drosophila. *Science* **238**, 1675-1681.

Panfilio, K. A., Oberhofer, G. and Roth, S. (2013). High plasticity in epithelial morphogenesis during insect dorsal closure. *Biol. Open* **2**, 1108-1118.

Paroush, Z., Wainwright, S. M. and Ish-Horowicz, D. (1997). Torso signalling regulates terminal patterning in Drosophila by antagonising Groucho-mediated repression. *Development* **124**, 3827-3834.

Patel, N. H., Kornberg, T. B. and Goodman, C. S. (1989). Expression of engrailed during segmentation in grasshopper and crayfish. *Development* **107**, 201-212.

Patel, N. H., Condron, B. G. and Zinn, K. (1994). Pair-rule expression patterns of even-skipped are found in both short- and long-germ beetles. *Nature* **367**, 429-434.

Richards, S., Gibbs, R. A., Weinstock, G. M., Brown, S. J., Denell, R., Beeman, R. W., Gibbs, R., Bucher, G., Friedrich, M., Grimmelikhuijzen, C. J. P. et al. (2008). The genome of the model beetle and pest Tribolium castaneum. *Nature* **452**, 949-955.

Rosenberg, M. I., Lynch, J. A. and Desplan, C. (2009). Heads and tails: Evolution of antero-posterior patterning in insects. *Biochim. Biophys. Acta* **1789**, 333-342.

Rusch, J. and Levine, M. (1994). Regulation of the dorsal morphogen by the Toll and torso signaling pathways: a receptor tyrosine kinase selectively masks transcriptional repression. *Genes Dev.* **8**, 1247-1257.

Rushlow, C., Frasch, M., Doyle, H. and Levine, M. (1987). Maternal regulation of zerknüllt: a homoeobox gene controlling differentiation of dorsal tissues in Drosophila. *Nature* **330**, 583-586.

Sarrazin, A. F., Peel, A. D. and Averof, M. (2012). A segmentation clock with two-segment periodicity in insects. *Science* **336**, 338-341.

Sato, K. and Siomi, M. C. (2015). Functional and structural insights into the piRNA factor Maelstrom. *FEBS Lett.* **589**, 1688-1693.

Sato, K., Nishida, K. M., Shibuya, A., Siomi, M. C. and Siomi, H. (2011). Maelstrom coordinates microtubule organization during Drosophila oogenesis through interaction with components of the MTOC. *Genes Dev.* **25**, 2361-2373.

Savant-Bhonsale, S. and Montell, D. J. (1993). torso-like encodes the localized determinant of Drosophila terminal pattern formation. *Genes Dev.* **7**, 2548-2555.

Schindelin, J., Arganda-Carreras, I., Frise, E., Kaynig, V., Longair, M., Pietzsch, T., Preibisch, S., Rueden, C., Saalfeld, S., Schmid, B. et al. (2012). Fiji: an open-source platform for biological-image analysis. *Nat. Methods* **9**, 676-682.

Schmitt-Engel, C., Cerny, A. C. and Schoppmeier, M. (2012). A dual role for nanos and pumilio in anterior and posterior blastodermal patterning of the short-germ beetle Tribolium castaneum. *Dev. Biol.* **364**, 224-235.

Schmitt-Engel, C., Schultheis, D., Schwirz, J., Ströhlein, N., Troelenberg, N., Majumdar, U., Dao, V. A., Grossmann, D., Richter, T., Tech, M. et al. (2015). The iBeetle large-scale RNAi screen reveals gene functions for insect development and physiology. *Nat. Commun.* **6**, 7822.

Schoppmeier, M. and Schröder, R. (2005). Maternal torso signaling controls body axis elongation in a short germ insect. *Curr. Biol.* **15**, 2131-2136.

Schroder, R., Eckert, C., Wolff, C. and Tautz, D. (2000). Conserved and divergent aspects of terminal patterning in the beetle Tribolium castaneum. *Proc. Natl. Acad. Sci. USA* **97**, 6591-6596.

St Johnston, D. and Ahringer, J. (2010). Cell polarity in eggs and epithelia: parallels and diversity. *Cell* **141**, 757-774.

St Johnston, D. and Nüsslein-Volhard, C. (1992). The origin of pattern and polarity in the Drosophila embryo. *Cell* **68**, 201-219.

Stevens, L. M., Beuchle, D., Jurcsak, J., Tong, X. and Stein, D. (2003). The Drosophila embryonic patterning determinant torsolike is a component of the eggshell. *Curr. Biol.* **13**, 1058-1063.

Tautz, D. and Pfeifle, C. (1989). A non-radioactive in situ hybridization method for the localization of specific RNAs in Drosophila embryos reveals translational control of the segmentation gene hunchback. *Chromosoma* **98**, 81-85.

van der Zee, M., Berns, N. and Roth, S. (2005). Distinct functions of the Tribolium zerknüllt genes in serosa specification and dorsal closure. *Curr. Biol.* **15**, 624-636.

van der Zee, M., Stockhammer, O., von Levetzow, C., Nunes da Fonseca, R. and Roth, S. (2006). Sog/Chordin is required for ventral-to-dorsal Dpp/BMP transport and head formation in a short germ insect. *Proc. Natl. Acad. Sci. USA* **103**, 16307-16312.

Van der Zee, M., da Fonseca, R. N. and Roth, S. (2008). TGFbeta signaling in Tribolium: vertebrate-like components in a beetle. *Dev. Genes Evol.* **218**, 203-213.

Wang, C. and Lehmann, R. (1991). Nanos is the localized posterior determinant in Drosophila. *Cell* **66**, 637-647.